



## **V2V-Assisted V2I MmWave Communication for Cooperative Perception with Information Value-Based Relay**

Downloaded from: <https://research.chalmers.se>, 2022-07-02 09:43 UTC

Citation for the original published paper (version of record):

Wu, P., Ding, L., Wang, Y. et al (2021). V2V-Assisted V2I MmWave Communication for Cooperative Perception with Information Value-Based Relay. GLOBECOM - IEEE Global Telecommunications Conference. <http://dx.doi.org/10.1109/GLOBECOM46510.2021.9685113>

N.B. When citing this work, cite the original published paper.

# V2V-Assisted V2I MmWave Communication for Cooperative Perception with Information Value-Based Relay

Peng Wu\*, Liqin Ding<sup>†</sup>, Yang Wang\*, Hui Zheng<sup>‡</sup>

\* School of Electronics and Information Engineering, Harbin Institute of Technology, Shenzhen, China

<sup>†</sup> Department of Electrical Engineering, Chalmers University of Technology, Gothenburg, Sweden

<sup>‡</sup> Ranplan Wireless Network Design Ltd, Cambridge, UK

Email: wupeng@stu.hit.edu.cn, yangw@hit.edu.cn

**Abstract**—Millimeter-wave (mmWave) vehicular communication is a key technology that enables autonomous vehicles to collaborate in environment perception, thereby improving traffic efficiency and safety to a new level. Many recent works have focused on relay-based solutions to overcome the inherent defects of mmWave, such as the severe path loss and its sensitivity to blockages. However, the selfishness of the vehicles is often ignored. Considering the application-oriented nature of vehicular communication, we propose an information value-based relay strategy for mmWave vehicle-to-infrastructure (V2I) transmission in this paper. Specifically, the vehicles are allowed to make relay decisions based on the evaluation of the value of messages from their own perspectives. To this end, a simple relay probability model based on the required awareness range is introduced. Through the use of stochastic geometry to model the vehicular network, the outage performance is analyzed and the results are validated by simulations. Impacts of both network and application related parameters on the outage performance are investigated. These preliminary results laid the foundation for the further expansion of the information value-based relay strategies to a wider range of network settings.

**Index Terms**—Vehicular relay, mmWave, selfish behavior, information value, stochastic geometry.

## I. INTRODUCTION

Cooperative environment perception achieved by sharing locally perceived environment information among autonomous vehicles (AVs) and roadside units (RSUs) is conceived as the key to a wide range of advanced safety and efficiency improving applications in future cooperative intelligent transportation systems (C-ITSs) [1], [2]. Through the vehicle-to-infrastructure (V2I) uplink transmission, AVs send the cooperative perception message (CPM) they generate to the RSUs. The collected CPMs are then fused locally at the RSUs or in a centralized manner at an edge server to which the RSUs are connected. Either way, the fused perception information is integrated into local dynamic map (LDM) messages, that are to be transmitted in the downlink to the AVs to help them better understand the surrounding environment. The LDM message required for a particular AV should contain information covering a sufficient awareness range of its surrounding environment so that C-ITS applications can be implemented.

The frequent exchange of sensing data requires very high data rates, stringent reliability, and ultra-low latency, which is a huge challenge to future vehicular networks. Due to the abundant bandwidth and high directional beamforming gain, millimeter wave (mmWave) communication is envisioned to play an important role [3]. However, when the line-of-sight (LOS) links are blocked by obstacles in the environment, mmWave vehicular communications will suffer severe performance loss. Therefore, relay-based transmission strategies have been considered in recent studies. For example, [4] proposes a traffic-aware relay vehicle selection scheme and [5] introduces a multi-hop V2V relaying method to improve the connecting performance of mmWave vehicle-to-vehicle (V2V) and V2I links. Most of the existing research is conducted under the obedient vehicle assumption, i.e., a vehicle will act as a relay whenever requested. This is, however, against the selfish nature of the vehicles in a realistic system, since relaying consumes energy, bandwidth, cache, and computing resources. To tackle this issue, a credit-based method was proposed in [6], in which a vehicle receives credits when it acts as relay and can only be relayed when it gathers enough credits. In [7], auction game theory is used to model the selfish behavior of vehicles, with each vehicle bidding for relaying to maximize its own profits.

In the context of cooperative perception, the message to be relayed also provides useful information for the relay vehicles. This is a distinctive feature of vehicular communications owing to its application-oriented nature and the shared safety-improving purpose. Considering the downlink LDM dissemination, in particular, the information contained in the LDM messages designated to nearby AVs is correlated, and the closer the AVs, the higher the correlation. Therefore, we propose an information value-based relay strategy to address the selfishness problem. This strategy allows the AVs to make relaying decisions based on the value of the information contained in their neighbors' LDM messages to them. To our best knowledge, this is the first attempt to consider the value of information in vehicular relay solutions.

In this paper, we adopt a simple relay probability model, which evaluates the information value based on the size of

the intersected area of the awareness ranges of the relaying vehicle and the destination vehicle. A tractable model for downlink LDM dissemination in a highway scenario is developed by using stochastic geometry, and the sectorized mmWave antenna array model is also taken into account. Exact expressions of outage probability are derived for both single- and double-relay transmissions, specifically resolving the effects of blockage correlation across cooperative V2I links [8]. The correctness of the analysis is verified by simulation. The impact of key parameters on the outage performance is also studied, such as AV density, blocking vehicle density, and the required awareness range of AVs.

## II. SYSTEM MODEL AND TRANSMISSION STRATEGY

We study the downlink LDM dissemination problem in a highway scenario. In particular, as shown in Fig. 1, a one-way  $N$ -lane road segment is considered. RSUs equipped with mmWave transceivers are deployed beside the outermost lane, and their distance to the edge of the road is given by  $0.5W$ , where  $W$  is the lane width. The most unfavorable situation is considered: the AVs drive in the innermost lane while the manned vehicles are traveling in the  $N-1$  outer lanes [9]. As a result, the manned vehicles become obstacles blocking the V2I links between AVs and RSUs. For the sake of simplicity, the manned vehicles and the AVs are referred to as the obstacles and the vehicles hereafter.

Each vehicle is associated with the closest RSU in the network. Due to the huge power loss, if the LOS link is blocked, it is considered that the transmission has failed. The neighboring vehicles can help to relay the LDM messages via the V2V links in case the direct V2I links are blocked. For V2V, it is assumed that LOS links only exist between adjacent vehicles [9] and that NLOS transmissions are also impenetrable. Based on these assumptions, the feasible transmission paths are limited to the following three cases:

- 1) V2I direct transmission: the target vehicle  $u_0$  receive LDM messages directly from its serving RSU  $b_0$ ;
- 2) Single-relay: when the V2I direct link is blocked, the nearest neighboring vehicle  $u_1$  serves as the relay node and forwards messages to  $u_0$  from  $b_0$ ;
- 3) Double-relay: when the V2I direct link is blocked, both neighboring vehicles  $u_1$  and  $u_2$  (one at each end of  $u_0$ ) act as relays and forward messages from  $b_0$  to  $u_0$ .

The time-frequency resources are divided into the same portions and used by the links to avoid interference.

### A. Information Value-Based Relay Decision Making

The required awareness range is assumed to be the same for all vehicles. In particular, the LDM message for a particular vehicle contains environmental information within the awareness range of  $c$  meters at both its front and back end. The larger the intersected area of the required awareness ranges of two vehicles, the higher the value of their packets is to the other. In the scenario considered in this paper, the size of the intersected area is proportional to the inter-vehicle distance. Hence, we allow vehicles to make relay decisions based on a

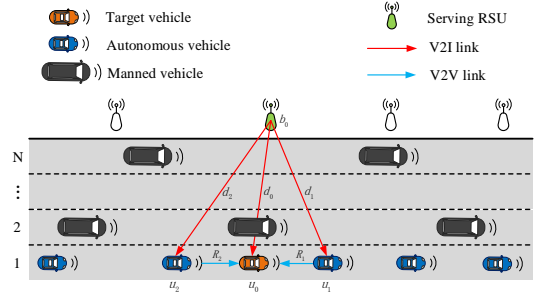


Fig. 1. The one-way  $N$ -lane highway scenario and the V2V-assisted V2I downlink transmission strategy.

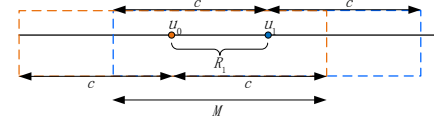


Fig. 2. An illustration of the information value-based relay probability model.

relay probability model that relies on the required awareness range of vehicles and the inter-vehicle distance.

Consider the single-relay case for an explanation. As shown in Fig. 2, we denote the inter-vehicle distance between  $u_0$  and  $u_1$  by  $R_1$  and the size of the overlapped region of the required awareness ranges of two vehicles by  $M$ . For  $u_1$ , the information value of the packet targeting  $u_0$  is given by  $\frac{M}{2c}$ . We then set the relay probability of  $u_1$  for  $u_0$  to the following:

$$P(R_1) = \begin{cases} 1 - \frac{R_1}{2c}, & 0 < R_1 \leq 2c \\ 0, & R_1 > 2c. \end{cases} \quad (1)$$

Namely,  $u_1$  assists  $u_0$  only when their required awareness ranges intersect. Note that the information value obtained in this paper is similar to the space awareness ratio (SAR) defined in [1] as one of the perception-related metrics. Similarly, the relay probability of  $u_2$  in the double-relay case is modeled in the same way.

### B. Stochastic Geometry-Based System Modeling

As in [10], the locations of RSUs and vehicles are modeled by two independent one-dimensional (1D) homogeneous Poisson point processes (HPPPs)  $\Phi_B$  and  $\Phi_U$  with densities  $\lambda_b$  and  $\lambda_u$ , respectively. The locations of obstacles are also modeled by multiple independent 1D HPPPs with the same density  $\lambda_k$ , and each obstacle is modeled by a segment of length  $l_k$ , while the widths and heights of obstacles are not part of our modeling. Without loss of generality,  $u_0$  is assumed to be located at the origin. Note that we only consider the snapshot of the highway vehicular network, without modeling vehicle mobility [9].

For the LOS channel model, we only consider a standard power-law path loss  $\omega_m(d) = A_m d^{-\alpha_m}$  [11], where  $\alpha_m$  is the path loss exponent,  $A_m$  is the reference path loss at a unit distance and  $m \in \{B, U\}$  is set to differentiate the V2I and V2V links, and  $d$  is the transmission distance between transceivers.

Since we consider the two-dimensional (2D) system model, a sectorized antenna array model which only contains the

antenna elements in the azimuth direction is introduced in this system [10]. Herein, the beamwidth and the main lobe gain of the antenna array are given by  $\theta_q$  and  $G_q$ , respectively. Note that  $q \in \{b, u\}$  is set to differentiate the RSU and vehicle. For simplicity, the transceivers of the desired link are assumed to complete the perfect beam alignment. In this system, we only consider the valid interfering RSUs which are subjected to two conditions: the paths from them to  $u_0$  are in LOS; their main beams cover  $u_0$ , and simultaneously they are covered by the main beam of  $u_0$  [12]. Note that there is no valid interference for V2V links since the main beam of  $u_0$  can only cover the neighboring vehicles on the same lane due to the narrow beamwidths employed in V2V communications. Additionally, the same frequency bandwidth  $B$  is allocated to all vehicles, and the half-duplex relay mode is adopted for the single-relay and double-relay transmission cases.

### C. Received Signals

Based on the above models, the received signal-to-interference-plus-noise ratio (SINR) at  $u_i$  ( $i \in \{0, 1, 2\}$ ) through the LOS V2I communication is given by

$$\text{SINR}_i = \frac{\omega_B(d_i)}{I_i + \sigma^2/(P_b G_b G_u)}, \quad (2)$$

where  $I_i = \sum_{j \in \Phi_{B_i} \setminus \{b_0\}} \omega_B(d_{ij})$  is the power of the normalized aggregate interference,  $d_i$  ( $d_{ij}$ ) is the transmission distance between  $b_0$  ( $b_j$ ) and  $u_i$ ,  $b_j$  is the  $j$ th interfering RSU,  $P_b$  is the transmitted power of RSUs, and  $Z$  is the additive white Gaussian noise (AWGN) with power  $\sigma^2$ ,  $\Phi_{B_i}$  is the set of valid interfering RSUs for  $u_i$ . Note that  $d_i = \sqrt{r_i^2 + y^2}$  and  $d_{ij} = \sqrt{r_{ij}^2 + y^2}$ , where  $r_i$  ( $r_{ij}$ ) is the 1D horizontal distance between  $b_0$  ( $b_j$ ) and  $u_i$ ,  $y$  is the 1D vertical distance between vehicles and RSUs, denoted by  $y = NW$ . For V2V communications, the received signal-to-noise ratio (SNR) at  $u_0$  transmitted by  $u_v$  ( $v \in \{1, 2\}$ ) is

$$\text{SNR}'_v = \frac{P_u G_u G_u \omega_U(R_v)}{\sigma^2}, \quad (3)$$

where  $R_v$  is the distance between  $u_v$  and  $u_0$ , and  $P_u$  is the transmitted power of vehicles.

## III. OUTAGE PROBABILITY ANALYSIS

The outage probability is adopted as the key performance metric in this paper. It is defined as the probability that no transmission link that can satisfy the required data rate  $T$  exists between  $u_0$  and  $b_0$ . Let  $K = 0, 1$ , and  $2$  denotes the direct transmission, single-relay, and double-relay cases respectively, and let  $C_0$ ,  $C_1$  and  $C_2$  denote the events that  $u_0$  can successfully receive the message by the single-hop V2I link and the two-hop V2I link using  $u_1$  or  $u_2$  for relaying, respectively. The outage probability of  $u_0$  is given by

$$P_{\text{out}}^K(T) = 1 - \mathbb{P}\left[\bigcup_{i=0}^K C_i\right]. \quad (4)$$

To derive the exact results of  $P_{\text{out}}$  by stochastic geometry, the effects of the blockage correlation across cooperative

V2I links are accounted for the single-relay and double-relay transmissions, i.e., a single obstacle can simultaneously block multiple V2I links.

### A. LOS Probability

For the clarified exposition, we define  $\mathbf{z}_i$  as the V2I link between  $u_i$  and  $b_0$ , and the sets  $\mathcal{V}_1 = \{\mathbf{z}_0, \mathbf{z}_1\}$ ,  $\mathcal{V}_2 = \{\mathbf{z}_0, \mathbf{z}_2\}$ ,  $\mathcal{V}_3 = \{\mathbf{z}_1, \mathbf{z}_2\}$  and  $\mathcal{V}_4 = \{\mathbf{z}_0, \mathbf{z}_1, \mathbf{z}_2\}$ .

**Lemma 1.** *The LOS probability of  $\mathbf{z}_0$  under the V2I direct transmission is given by*

$$P_0 = \exp(-\lambda_k l_k (N-1)). \quad (5)$$

*Proof.* The proof follows [10] and is omitted here.  $\square$

**Proposition 1.** *Given that  $u_1$  and  $u_2$  are the deterministic relays of  $u_0$  and the inter-vehicle distance  $R_1$  and  $R_2$  are known under the single-relay and double-relay transmissions, the joint LOS probabilities of the V2I links in  $\mathcal{V}_1$ ,  $\mathcal{V}_2$ ,  $\mathcal{V}_3$  and  $\mathcal{V}_4$  are respectively given by*

$$P_{\text{LOS}}(\mathcal{V}_1|R_1) = Q_1(R_1), \quad (6)$$

$$P_{\text{LOS}}(\mathcal{V}_2|R_2) = Q_1(R_2), \quad (7)$$

$$P_{\text{LOS}}(\mathcal{V}_3|R_1, R_2) = Q_1(R_1 + R_2), \quad (8)$$

$$P_{\text{LOS}}(\mathcal{V}_4|R_1, R_2) = Q_2(R_1, R_2), \quad (9)$$

where we define that

$$Q_1(x) = \prod_{n=1}^{N-1} \exp\left(-\lambda_k \left(l_k + \min\left(\frac{(N-n)x}{N}, l_k\right)\right)\right), \quad (10)$$

$$Q_2(x_1, x_2) = \prod_{n=1}^{N-1} \exp\left(-\lambda_k \left(l_k + \min\left(\frac{(N-n)x_1}{N}, l_k\right) + \min\left(\frac{(N-n)x_2}{N}, l_k\right)\right)\right). \quad (11)$$

*Proof.* See Appendix A.  $\square$

### B. Outage Probability

In this subsection, the outage probability  $P_{\text{out}}$  is characterized by using the dominant interference analysis method [13], which only considers the interferer that can cause an outage at the receiver without the participation of other interferers.

**Lemma 2.** *Given the rate threshold  $T$ , the outage probability of  $u_0$  under the V2I direct transmission is given by*

$$P_{\text{out}}^0(T) = 1 - 2\lambda_b P_0 \int_0^\infty e^{-2\lambda_b r_0 - \beta \rho(\tau_1, r_0)} dr_0. \quad (12)$$

Herein,  $\rho(x_1, x_2) = 2\lambda_b P_0 (D(x_1, x_2) - r_0)$ ,  $D(x_1, x_2) = \sqrt{\left(\frac{(x_1^2 + x_2^2) - \frac{\alpha_B}{2}}{x_1} - \frac{\sigma^2}{P_b A_B G_b G_u}\right)^{-\frac{2}{\alpha_B}} - y^2}$ ,  $\beta = \frac{\theta_b^H \theta_u^H}{\pi^2}$ , and  $\tau_1 = 2^{\frac{T}{B}} - 1$ .

*Proof.* See Appendix B.  $\square$

**Theorem 1.** *Given the rate threshold  $T$ , the outage probabilities of  $u_0$  under the single-relay and double-relay transmissions are given by (13) and (14) respectively, shown at the bottom of the next page, where we define that*

$$\eta_1(x) = 0.5e^{-\beta\rho(\tau_2, x+r_0)} + 0.5e^{-\beta\rho(\tau_2, x-r_0)}, \quad (15)$$

$$\eta_2(x) = 0.5e^{-\beta\rho(\tau_3, x+r_0)} + 0.5e^{-\beta\rho(\tau_3, x-r_0)}, \quad (16)$$

$$\begin{aligned} \eta_3(x_1, x_2) &= 0.5e^{-\beta(\rho(\tau_2, x_1+r_0)+\rho(\tau_3, x_2-r_0))} \\ &+ 0.5e^{-\beta(\rho(\tau_2, x_1-r_0)+\rho(\tau_3, x_2+r_0))}. \end{aligned} \quad (17)$$

Herein,  $\tau_2 = 2^{\frac{2T}{B}} - 1$ ,  $c_1 = \min\left(2c, \left(\frac{P_u G_u G_u A_u}{\tau_2 \sigma^2}\right)^{\frac{1}{\alpha_u}}\right)$ ,  $\tau_3 = 2^{\frac{3T}{B}} - 1$ ,  $c_2 = \min\left(2c, \left(\frac{P_u G_u G_u A_u}{\tau_3 \sigma^2}\right)^{\frac{1}{\alpha_u}}\right)$ ,  $f(R_1)$  and  $f(R_2)$  are the probability density functions (PDFs) of  $R_1$  and  $R_2$  respectively, given by  $f(R_1) = 2\lambda_u e^{-2\lambda_u R_1}$  and  $f(R_2) = 2\lambda_u (e^{-\lambda_u R_2} - e^{-2\lambda_u R_2})$ , and  $f(R_1, R_2)$  is the joint PDF of  $R_1$  and  $R_2$ , given by  $f(R_1, R_2) = 2\lambda_u^2 e^{-\lambda_u(R_1+R_2)}$ .

*Proof.* See Appendix C.  $\square$

**Remark 1.** Under the assumption of independent blockage between cooperative V2I links as in [14], the simplified outage probabilities  $\bar{P}_{\text{out}}^1(T)$  and  $\bar{P}_{\text{out}}^2(T)$  can be obtained by substituting  $P_{\text{LOS}}(\mathcal{V}_1|R_1)$ ,  $P_{\text{LOS}}(\mathcal{V}_2|R_2)$ ,  $P_{\text{LOS}}(\mathcal{V}_3|R_1, R_2)$  with  $\exp(-2\lambda_k l_k(N-1))$ , and  $P_{\text{LOS}}(\mathcal{V}_4|R_1, R_2)$  with  $\exp(-3\lambda_k l_k(N-1))$  in (13) and (14) respectively.

#### IV. NUMERICAL RESULTS AND DISCUSSION

In what follows, the outage performance is studied through Monte Carlo (MC) simulations in a typical highway scenario. Unless otherwise stated, we choose following [15]:  $\lambda_b = 10$  RSUs/km,  $\lambda_u = 20$  vehicles/km,  $\lambda_k = 10$  vehicles/km,  $N = 2$ ,  $W = 3.5$  m,  $l_k = 12$  m,  $c = 100$  m,  $\alpha_b = 2.2$ ,  $\alpha_u = 2$ ,  $A_b = 10^{-12.3}$ ,  $A_u = 10^{-12.14}$ ,  $G_b = 20$  dB,  $G_u = 10$  dB,  $\theta_b = 30^\circ$ ,  $B = 100$  MHz,  $T = 200$  Mbps,  $P_b = 27$  dBm,  $P_v = 24$  dBm, and  $-174$  dBm/Hz for the noise power spectral density. Note that we set  $\theta_u = 36^\circ$  for V2I communications but set  $\theta_u = 5^\circ$  for V2V communications. For the sake of clarity, we use ‘NC’ to abbreviate ‘no-correlation’ in the legends of the figures.

Fig. 3 validates the analytical results of  $P_{\text{out}}$  by MC simulations. The analytical results match well with the simulated results in general. One can observe a small gap between them that increases with  $T$ , and is clearer in the double-relay transmission case. The analytical results are always smaller than the simulated results, which is due to the fact that we only take the dominant interferers into account in the analyses and further cause the underestimation of the aggregate interference power and the outage probability. The impact of the simplified interference analysis becomes more

obvious with a larger  $T$  and when more relay nodes are adopted. The V2V-assisted transmission schemes contribute to improving the outage performance due to the introduced diversity gain, as compared with the V2I direct transmission. Additionally,  $P_{\text{out}}$  deteriorates with the increased number of lanes  $N$  since there are more obstacles to block the V2I links.

Fig. 4(a) and Fig. 4(b) depict the impacts of the obstacle density  $\lambda_k$  and the vehicle density  $\lambda_u$  on  $P_{\text{out}}$  respectively. It is clear that  $P_{\text{out}}$  increases with  $\lambda_k$  regardless of the transmission strategies being adopted, since the LOS probabilities of all the V2I links decreases. With the increase of  $\lambda_u$ ,  $P_{\text{out}}$  is a constant under the V2I direct transmission, while in the single- and double-relay transmission cases,  $P_{\text{out}}$  firstly decreases and then increases after reaching the bottom. This is because the inter-vehicle distance shrinks as  $\lambda_u$  grows, which leads to higher relay probabilities at the neighboring vehicles on one hand, and higher correlations between the cooperative V2I links on the other hand, which degrades the diversity gain. When  $\lambda_u$  becomes large enough, the diversity gain degradation becomes the dominating effect. Besides the exact analytical results, the approximate results based on the no-correlation assumption of blockage between cooperative V2I links are also presented in Fig. 4. The curves clearly show that the no-correlation assumption, which exaggerates the diversity gain, results in not only overly optimistic outage performance predictions, but also false trends in the  $P_{\text{out}}$  curves against  $\lambda_u$ . This indicates that the impact of blockage correlation cannot be neglected especially under dense vehicle situations.

In Fig. 5, we investigate the impact of the required awareness range  $c$  on the outage probability  $P_{\text{out}}$  for the single-relay transmission. It is observed that  $P_{\text{out}}$  decreases with the increase of  $c$ , since a larger  $c$  leads to a higher relay probability at the neighboring vehicle when the inter-vehicle distance remains unchanged. More importantly, the vehicle density which leads to the minimum  $P_{\text{out}}$ , decreases as  $c$  grows. The reason is that when  $c$  is large enough, the relay probability of the neighboring vehicle would approach 1 even if  $\lambda_u$  is small. The outage performance achieved with the totally altruistic relay assumption (with relay probability always being 1) is also plotted. In this case,  $P_{\text{out}}$  increases monotonically with  $\lambda_u$  and is always smaller than that with the selfish relay, since the selfishness of vehicles would cause less cooperation between the target vehicle and its neighboring vehicle, and further result in the smaller diversity gain. Moreover, the performance gap is small when both  $\lambda_u$  and  $c$  are large, since the vehicles are

$$P_{\text{out}}^1(T) = 1 - 2\lambda_b \int_0^\infty e^{-2\lambda_b r_0} \left( P_0 e^{-\beta\rho(\tau_1, r_0)} + \int_0^{c_1} f(R_1) P(R_1) \eta_1(R_1) (P_0 - P_{\text{LOS}}(\mathcal{V}_1|R_1) e^{-\beta\rho(\tau_1, r_0)}) dR_1 \right) dr_0. \quad (13)$$

$$\begin{aligned} P_{\text{out}}^2(T) &= 1 - 2\lambda_b \int_0^\infty e^{-2\lambda_b r_0} \left( P_0 e^{-\beta\rho(\tau_1, r_0)} + \int_0^{c_1} f(R_1) P(R_1) \eta_1(R_1) (P_0 - P_{\text{LOS}}(\mathcal{V}_1|R_1) e^{-\beta\rho(\tau_1, r_0)}) dR_1 \right. \\ &+ \int_0^{c_2} f(R_2) P(R_2) \eta_2(R_2) (P_0 - P_{\text{LOS}}(\mathcal{V}_2|R_2) e^{-\beta\rho(\tau_1, r_0)}) dR_2 + \int_0^{c_2} \int_0^{R_2} f(R_1, R_2) P(R_1) P(R_2) \\ &\left. \times \eta_3(R_1, R_2) (e^{-\beta\rho(\tau_1, r_0)} P_{\text{LOS}}(\mathcal{V}_4|R_1, R_2) - P_{\text{LOS}}(\mathcal{V}_3|R_1, R_2)) dR_1 dR_2 \right) dr_0. \end{aligned} \quad (14)$$

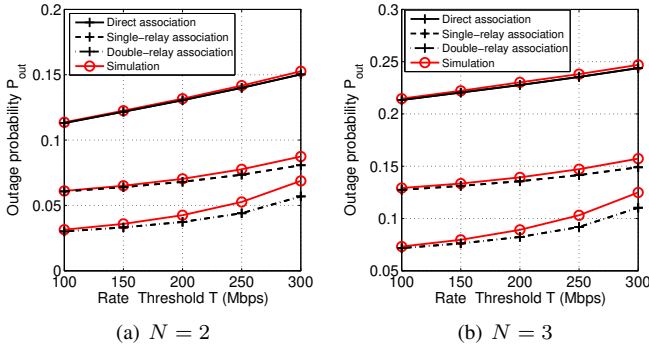


Fig. 3. Validation of analytical results of  $P_{\text{out}}$  with MC simulations.

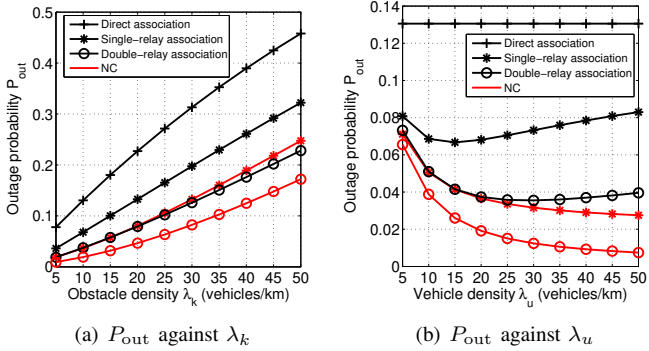


Fig. 4. Comparison between exact analytical results and simplified non-correlation results of  $P_{\text{out}}$ .

more willing to forward the LDM messages for their neighbors thanks to the increasing of information value to them.

## V. CONCLUSIONS AND FUTURE WORKS

In this paper, we have proposed an information value-based relay strategy for the cooperative perception-oriented mmWave V2I downlink transmission and investigated the impacts of both network and application related parameters on the outage performance. Specifically, we have considered the contribution of the forwarded messages to the awareness range requirements of vehicles, and addressed the selfishness problem of vehicles by introducing an information value-based relay probability model. A tractable analysis framework has been developed to derive the expressions of outage probability in both single- and double-relay transmission cases, which resolves the effects of blockage correlation among V2I links for analysis accuracy, and the impact of the selfishness of vehicles on the outage performance has been evaluated numerically.

For future works, the information value-based relay strategy will be extended to a wider range of transmission scenarios in mmWave vehicular networks, and the relay probability model will be modified accordingly. Novel performance metrics are also needed for appropriate performance evaluation at the system level.

## ACKNOWLEDGMENT

This work was supported in part by the National Key R&D Program of China under Grant 2017YFE0118900, in

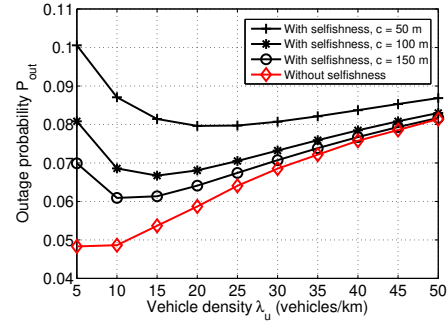


Fig. 5. Outage probability  $P_{\text{out}}$  against  $\lambda_u$  in the single-relay transmission case with various  $c$ .

part by H2020-MSCA-IF Grant 887732 (VoiiComm), in part by the Marine Economy Development Project of Guangdong Province under Grant GDNRC [2020] 014 and GDNRC [2020] 026, in part by the "Innovation Chain + Industry Chain" Project of Shenzhen under Grant 20190830020005, and in part by the Science and Technology Project of Shenzhen under Grant JCYJ20200109113424990.

## APPENDIX

### A. Proof of Proposition 1

Let  $S_1(n)$ ,  $S_2(n)$ ,  $S_3(n)$  and  $S_4(n)$  respectively denote the length of joint blockage area on the  $n$ th ( $1 \leq n \leq N_B$ ) blockage lane for all links in  $\mathcal{V}_1$ ,  $\mathcal{V}_2$ ,  $\mathcal{V}_3$  and  $\mathcal{V}_4$ . We firstly obtain  $S_1(n)$  by the geometrical relationship shown in Fig. 6. If the two blockage areas are overlapping,  $S_1(n) = L_1(n) + l_k$ , otherwise, we have  $S_1(n) = 2l_k$ . Herein,  $L_1(n)$  is the distance between two points of intersection of  $\mathbf{z}_0$ ,  $\mathbf{z}_1$  and the  $n$ -th blockage lane, denoted by  $L_1(n) = \frac{(N-n)R_1}{N}$ . Hence, we have

$$S_1(n) = l_k + \min\left(\frac{(N-n)R_1}{N}, l_k\right). \quad (18)$$

Further, by using the void probability of the PPPs and the independence of blockages on different lanes, the joint LOS probability of  $\mathbf{z}_0$  and  $\mathbf{z}_1$  is given by

$$P_{\text{LOS}}(\mathcal{V}_1 | R_1) = \prod_{n=1}^{N-1} \exp(-\lambda_k S_1(n)) = Q_1(R_1). \quad (19)$$

Like the method to obtain  $S_1(n)$ , we can get  $S_2(n)$ ,  $S_3(n)$  and  $S_4(n)$ , and hence obtain the results of (7), (8) and (9).

### B. Proof of Lemma 2

According to (4), we have

$$\begin{aligned} P_{\text{out}}^0(T) &= 1 - \mathbb{P}[B \log_2(1 + \text{SINR}_0) > T] \\ &= 1 - \mathbb{P}[\text{SINR}_0 > \tau_1], \end{aligned} \quad (20)$$

where  $\tau_1 = 2^{T/B} - 1$ . Note that  $\mathbb{P}[\text{SINR}_0 > \tau_1]$  is the probability that  $\mathbf{z}_0$  is in LOS and simultaneously  $\text{SINR}_0$  is larger than  $\tau_1$ . Hence, we get

$$\begin{aligned} \mathbb{P}[\text{SINR}_0 > \tau_1] &= \mathbb{P}[\text{SINR}_0 > \tau_1 | \text{LOS}] P_0 \\ &= \int_0^\infty \mathbb{P}\left[\frac{\omega_B(\sqrt{r_0^2 + y^2})}{I_0 + \sigma^2/(P_b G_b G_u)} > \tau_1\right] P_0 f(r_0) dr_0, \end{aligned} \quad (21)$$

where  $f(r_0)$  is the PDF of  $r_0$ , given by  $f(r_0) = 2\lambda_b e^{-2\lambda_b r_0}$ .

Based on the dominant interferer analysis, we have

$$\begin{aligned}
& \mathbb{P}\left[\frac{\omega_B(\sqrt{r_0^2 + y^2})}{I_0 + \sigma^2/(P_b G_b G_u)} > \tau_1\right] \\
&= \mathbb{P}\left[I_0 < \frac{A_B(r_0^2 + y^2)^{-\frac{\alpha_B}{2}}}{\tau_1} - \frac{\sigma^2}{P_b G_b G_u}\right] \\
&\leq \mathbb{P}\left[d_{0j}^{-\alpha_B} < \frac{(r_0^2 + y^2)^{-\frac{\alpha_B}{2}}}{\tau_1} - \frac{\sigma^2}{A_B P_b G_b G_u}\right] \\
&= \mathbb{P}\left[d_{0j} > \left(\frac{(r_0^2 + y^2)^{-\frac{\alpha_B}{2}}}{\tau_1} - \frac{\sigma^2}{A_B P_b G_b G_u}\right)^{-\frac{1}{\alpha_B}}\right] \\
&= \mathbb{P}[r_{0j} > D(\tau_1, r_0)], \tag{22}
\end{aligned}$$

where the inequality in the third line follows from the fact that we only consider the interference from the single RSU  $b_j$  rather than the aggregate interference. Therefore, the set of dominant interfering RSUs  $\Phi'_{B_0}$  contains the interfering RSU, such as  $b_j$ , which is subjected to three conditions: 1) the V2I link between  $b_j$  and  $u_0$  is in LOS; 2)  $b_j$  is covered by the main beam of  $u_0$  and its main beam also covers  $u_0$ ; 3)  $r_{0j} \leq D(\tau_1, r_0)$ .

For condition 1, the LOS probability between  $b_j$  and  $u_0$  is given by  $P_0$ . The probability of condition 2 is obtained by  $P_{H_b} P_{H_u} = \frac{\theta_b^H \theta_u^H}{\pi^2}$ . Therefore, the average number of RSUs which belong to  $\Phi'_{B_0}$  is given by

$$\begin{aligned}
\Lambda_b &= \int_{r_0}^{D(\tau_1, r_0)} 2\lambda_b P_0 P_{H_b} P_{H_u} dx \\
&= 2\lambda_b e^{-\lambda_k l_k(N-1)} \frac{\theta_b^H \theta_u^H}{\pi^2} (D(\tau_1, r_0) - r_0). \tag{23}
\end{aligned}$$

Based on stochastic geometry, we get

$$\mathbb{P}[\text{SINR}_0 > \tau_1] = \int_0^\infty \exp(-\Lambda_b) P_0 f(r_0) dr_0. \tag{24}$$

Finally, substituting (24) into (20), (12) is obtained.

### C. Proof of Theorem 1

According to (4) and the inclusion-exclusion formula, we get

$$P_{\text{out}}^1(T) = 1 - \mathbb{P}[C_0] - \mathbb{P}[C_1] + \mathbb{P}[C_0 \cap C_1], \tag{25}$$

where  $\mathbb{P}[C_0]$  is derived by  $1 - P_{\text{out}}^0(T)$  from Lemma 2. For  $\mathbb{P}[C_1]$ , we have

$$\begin{aligned}
\mathbb{P}[C_1] &= \mathbb{P}[0.5B \log_2(1 + \min(\text{SINR}_1, \text{SNR}'_1)) > T] \\
&= \mathbb{P}[\min(\text{SINR}_1, \text{SNR}'_1) > \tau_2] \tag{26}
\end{aligned}$$

where  $\tau_2 = 2^{\frac{2T}{B}} - 1$ . Note that  $\mathbb{P}[\min(\text{SINR}_1, \text{SNR}'_1) > \tau_2]$  is the probability that  $u_1$  can be the relay of  $u_0$ , and  $\mathbf{z}_1$  is in LOS, and  $\text{SINR}_1$  and  $\text{SNR}'_1$  are both larger than  $\tau_2$ . Hence,

$$\begin{aligned}
\mathbb{P}[\min(\text{SINR}_1, \text{SNR}'_1) > \tau_2] &= \\
&\int_0^\infty \int_0^{2c} f(r_0) f(R_1) P(R_1) P_0 \mathbb{P}[\text{SINR}_1 > \tau_2 | \text{LOS}, r_0, R_1] \\
&\quad \mathbb{P}[\text{SNR}'_1 > \tau_2 | R_1] dR_1 dr_0. \tag{27}
\end{aligned}$$

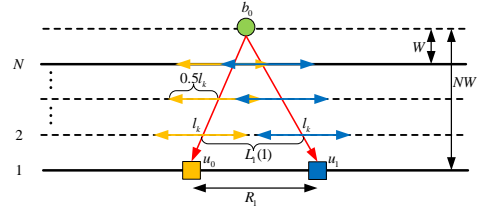


Fig. 6. Illustration of the blockage area for cooperative V2I links of  $u_0$ .

By using the same method shown in Appendix B, we can derive  $\mathbb{P}[\text{SINR}_1 > \tau_2 | \text{LOS}, r_0, R_1]$  and  $\mathbb{P}[\text{SNR}'_1 > \tau_2 | R_1]$ , and further obtain  $\mathbb{P}[C_1]$ . Similarly, we can derive the result of  $\mathbb{P}[C_0 \cap C_1]$  and further obtain  $P_{\text{out}}^1(T)$  as shown in (13).

By the same analogy,  $P_{\text{out}}^2(T)$  can be obtained, which is omitted here due to the limited space.

### REFERENCES

- [1] F. Schiegg, I. Llatser, D. Bischoff, and G. Volk, "Collective perception: A safety perspective," *Sensors*, vol. 21, no. 1, pp. 1–23, Dec. 2020.
- [2] L. Ding, Y. Wang, P. Wu, L. Li, and J. Zhang, "Kinematic information aided user-centric 5G vehicular networks in support of cooperative perception for automated driving," *IEEE Access*, vol. 7, pp. 40195–40209, 2019.
- [3] M. Fallgren *et al.*, "Fifth-generation technologies for the connected car: Capable systems for vehicle-to-anything communications," *IEEE Veh. Technol. Mag.*, vol. 13, no. 3, pp. 28–38, Sep. 2018.
- [4] B. Fan, H. Tian, S. Zhu, Y. Chen, and X. Zhu, "Traffic-aware relay vehicle selection in millimeter-wave vehicle-to-vehicle communication," *IEEE Wireless Commun. Lett.*, vol. 8, no. 2, pp. 400–403, Apr. 2019.
- [5] A. Taya *et al.*, "Coverage expansion through dynamic relay vehicle deployment in mmwave V2I communications," in *Proc. IEEE Veh. Tech. Conf. (VTC)*, Jul. 2018, pp. 1–5.
- [6] T. Chen, L. Zhu, F. Wu, and S. Zhong, "Stimulating cooperation in vehicular ad hoc networks: A coalitional game theoretic approach," *IEEE Trans. Veh. Technol.*, vol. 60, no. 2, pp. 566–579, Nov. 2011.
- [7] Y. Hui, Z. Su, T. H. Luan, and J. Cai, "Content in motion: An edge computing based relay scheme for content dissemination in urban vehicular networks," *IEEE Trans. Intell. Transp. Syst.*, vol. 20, no. 8, pp. 3115–3128, Aug. 2019.
- [8] P. Wu, L. Ding, Y. Wang, L. Li, H. Zheng, and J. Zhang, "Performance analysis for uplink transmission in user-centric ultra-dense V2I networks," *IEEE Trans. Veh. Technol.*, vol. 69, no. 9, pp. 9342–9355, 2020.
- [9] W. Yi, Y. Liu, Y. Deng, A. Nallanathan, and R. W. Heath, "Modeling and analysis of mmwave V2X networks with vehicular platoon systems," *IEEE J. Sel. Areas Commun.*, vol. 37, no. 12, pp. 2851–2866, Dec. 2019.
- [10] A. Tassi, M. Egan, R. J. Piechocki, and A. Nix, "Modeling and design of millimeter-wave networks for highway vehicular communication," *IEEE Trans. Veh. Technol.*, vol. 66, no. 12, pp. 10676–10691, Dec. 2017.
- [11] D. Yan *et al.*, "Channel characterization for vehicle-to-infrastructure communications in millimeter-wave band," *IEEE Access*, vol. 8, pp. 42325–42341, Feb. 2020.
- [12] A. Shafie, N. Yang, Z. Sun, and S. Durrani, "Coverage analysis for 3D Terahertz communication systems with blockage and directional antennas," in *Proc. IEEE Int. Conf. on Commun. (ICC Workshops)*, Jun. 2020, pp. 1–7.
- [13] S. Wu, R. Atar, N. Mastrorarde, and L. Liu, "Improving the coverage and spectral efficiency of millimeter-wave cellular networks using device-to-device relays," *IEEE Trans. Commun.*, vol. 66, no. 5, pp. 2251–2265, May. 2018.
- [14] C. Tunc *et al.*, "The blind side: Latency challenges in millimeter wave networks for connected vehicle applications," *IEEE Trans. Veh. Technol.*, vol. 70, no. 1, pp. 529–542, Jan. 2021.
- [15] 3GPP, TR 37.885 v15.3.0, "Study on evaluation methodology of new vehicle-to-everything (V2X) use cases for LTE and NR," Jun. 2019.